Supporting Information

Simultaneous electrodeposition of manganese oxide/poly(o-aminophenol) composites as the electrode material for aqueous electrochemical energy storage

Shaotong Pei[a,*], Bo Lan[a], Xueting Bai[a], Yunpeng Liu[a], Xinlan Yi[b], Haichao Sun[a], Weiqi Wang[a], Mianxiao Wu [a], Chao Wang[c,d,*]

a. *Hebei Provincial Key Laboratory of Power Transmission Equipment Security Defense, North China Electric Power University, Baoding, Hebei 071003, China*
b. *Economic management Department, North China Electric Power University, Baoding, Hebei 071003, China*
c. *School of Renewable Energy, Inner Mongolia University of Technology, Ordos, Inner Mongolia 017010, China*
d. *Inner Mongolia Key Laboratory of New Energy and Energy Storage Technology, Hohhot 010051, China*

Corresponding authors:

peishaotong@ncepu.edu.cn
cwang@imut.edu.cn

Contents

1. Experimental

Chemicals

The following reagents were used without further purification: Manganese sulfate ($MnSO_4 \cdot H_2O$, AR, 99.0%, FuChen (Tianjin) Chemical Reagents Co., Ltd.), *o*-aminophenol (C_6H_7NO, AR, 99%, Shanghai Aladdin Biochemical Technology Co., Ltd.), concentrated sulfuric acid (H_2SO_4, AR, 98.0%, Shanghai HaoHong Bio-Pharmaceutical Technology Co., Ltd.), zinc sulfate ($ZnSO_4$, AR, 99.8%, Shanghai HaoHong Bio-Pharmaceutical Technology Co., Ltd.), potassium chloride (KCl, AR, 99.5%, FuChen (Tianjin) Chemical Reagents Co., Ltd.), potassium ferricyanide ($K_3[Fe(CN)_6]$, AR, 99.5%, Tianjin RuiJinTe Chemicals Co., Ltd.), ammonium sulfate ($(NH_4)_2SO_4$, AR, 99.1%, Shanghai BiDe Pharmaceutical Technology Co., Ltd.), carbon cloth (SCC130, Suzhou ShengErNuo Technology Co., Ltd.) and doubly distilled water.

Instrumentation

X-ray photoelectron spectroscopy was performed on Shimadzu/Krayos AXIS Ultra DLD at room temperature and ultra-high vacuum (UHV) conditions. The full-spectrum acquisition voltage was 15 kV, filament current was 5 mA, and the test pass energy Pass Energy was 160ev; the fine-spectrum voltage was 15 kV, filament current was 10 mA, and the test pass energy Pass Energy was 40eV. Charge correction was performed using C 1s=284.80 eV binding energy as the energy standard.X-ray diffraction (XRD) was performed on X-ray powder diffractometer (Rigaku SmartLab SE, Japan) equipped with a Cu target (λ = 0.154 nm). Field emission scanning electron microscope (ZEISS Sigma 300, Germany) equipped with electron diffraction spectroscope was used to observe the morphology and elemental distribution of the film.

Electrochemistry

The electrochemical measurements are carried out at room temperature using CHI760E electrochemical workstation, and EIS was recorded in the frequency range of 10^6 to 0.01 Hz under potential amplitude 5 mV. The specific capacity (C, mAh g^{-1}) was calculated from the discharge branch of the GCD curve by the following formula.

$$C_{S,GCD} = \frac{It}{m} \quad (1)$$

Where I (mA) is the discharge current, t (h) is the discharge time, and m (g) is the mass of the active material on the electrode. The specific capacity (C, mAh g^{-1}) is also calculated based on the integrated charge (Q, C) obtained from the CV cathodic scan by the following formula.

$$C_{S,CV} = \frac{Q}{3.6m} \quad (2)$$

The capacitance of the MnO_x/PoAP two-electrode energy storage system was calculated from the GCD curve using Equation (3).

$$C_{cell} = \frac{It}{2m \times \Delta V} \quad (3)$$

Where C_{cell}(F g^{-1}) is the specific capacity based on the mass of electrochemically active material,

I is the current in A, and ΔV(V) is the potential window.

The energy density and power density of the solid-state supercapacitor were calculated using Equations (4) and (5).

$$E = \frac{1}{2 \times 3.6 \times 2m} \int_0^t V dt \quad (4)$$

$$P = \frac{E \times 3600}{t} \quad (5)$$

where E ($Wh\ kg^{-1}$) and P ($W\ kg^{-1}$) correspond to energy density and power density, respectively.

2. Electrochemistry

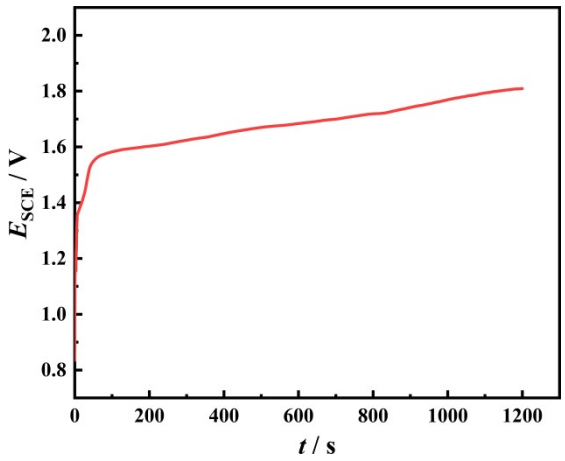

Figure S1. *E* - *t* curve for electropolymerization in 10 mM $MnSO_4$ + 1 mM PoAP + 1 M H_2SO_4 at 0.014 A cm^{-2}. The working electrode is CC.

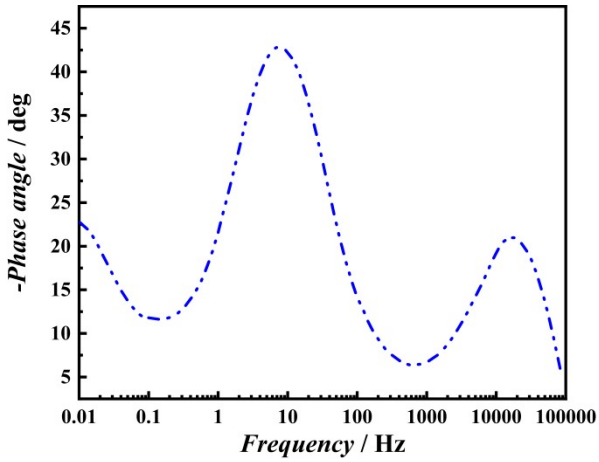

Figure S2. Bode plot of symmetric supercapacitor with 2 M $(NH_4)_2SO_4$ aqueous electrolyte.

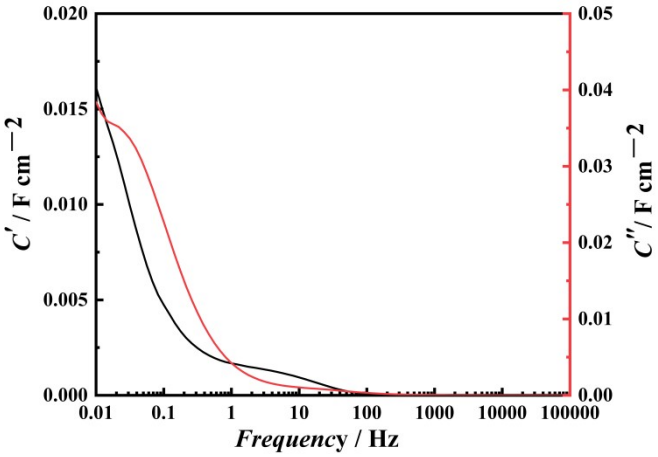

Figure S3. Plots of *C*' and *C*'' *vs. f* of the symmetric supercapacitor with 2 M $(NH_4)_2SO_4$ aqueous electrolyte.

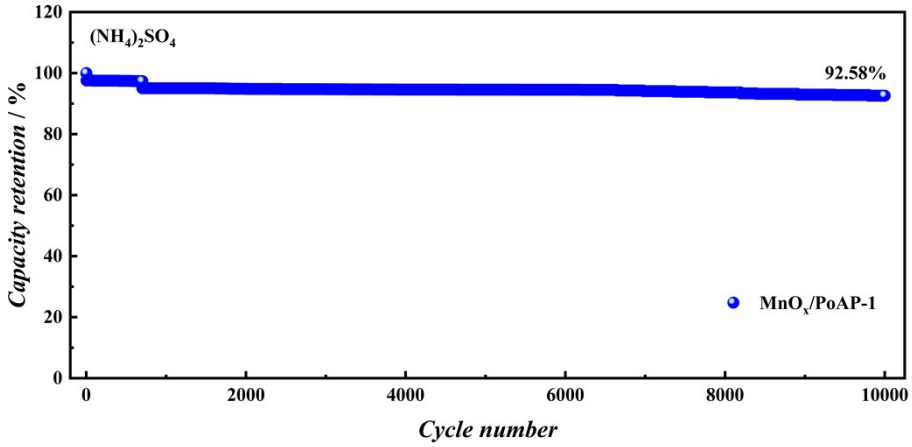

Figure S4. The cycling stability of MnO_x/PoAP-1 at 10 A g^{-1} in 2 M $(NH_4)_2SO_4$.

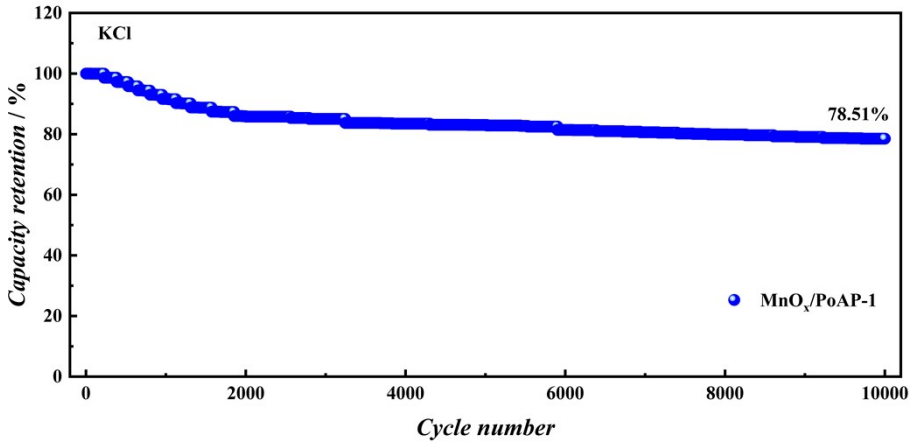

Figure S5. The cycling stability of MnO_x/PoAP-1 at 10 A g^{-1} in 2 M KCl.

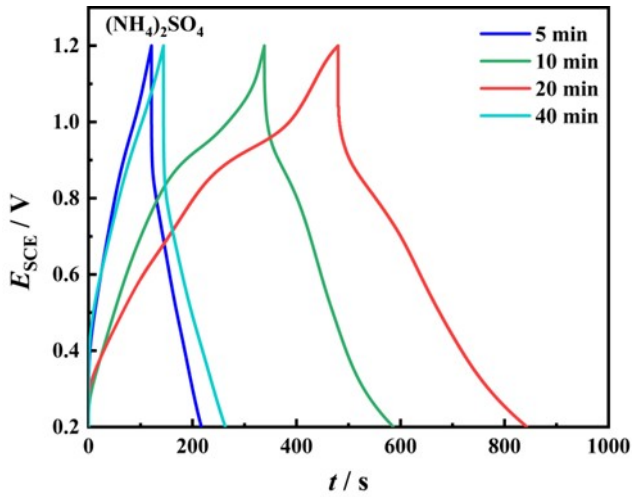

Figure S6. GCD profiles of MnO_x/PoAP obtained by electrochemical deposition at different times for 14 $mAcm^{-2}$.

3. XPS

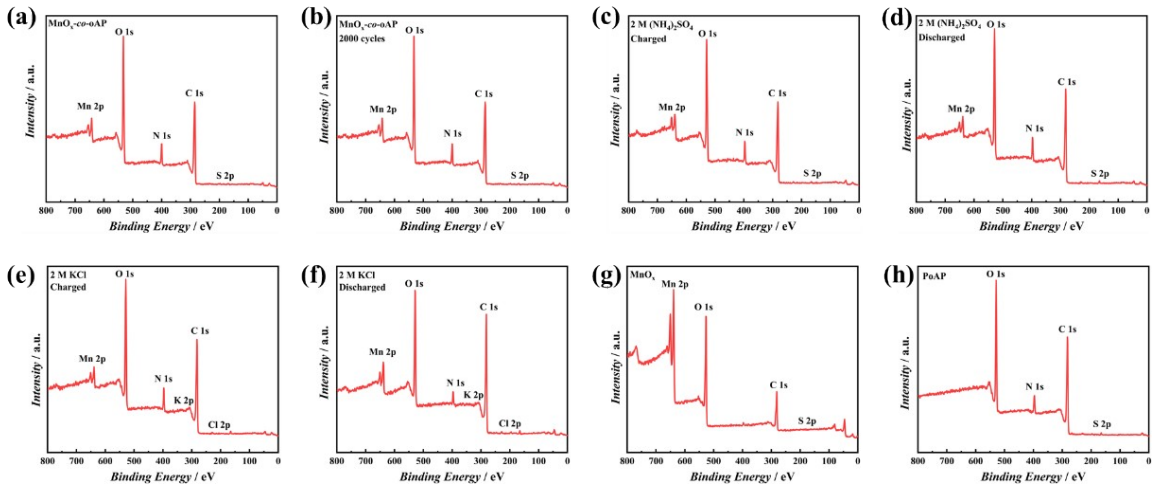

Figure S7. (a) XPS survey spectrum of the MnO_x/PoAP-1; XPS survey spectrum of the MnO_x/PoAP-1 under various conditions (b) after charge-discharge 2000 cycles in 2 M $(NH_4)_2SO_4$ (c) Charged to 1.2 V_{SCE} in 2 M $(NH_4)_2SO_4$ (d) Discharged to 0.2 V_{SCE} in 2 M $(NH_4)_2SO_4$ (e) Charged to 1.0 V_{SCE} in 2 M KCl (f) Discharged to −0.5 V_{SCE} in 2 M KCl; XPS survey spectrum of the (g) MnO_x and (h) PoAP.

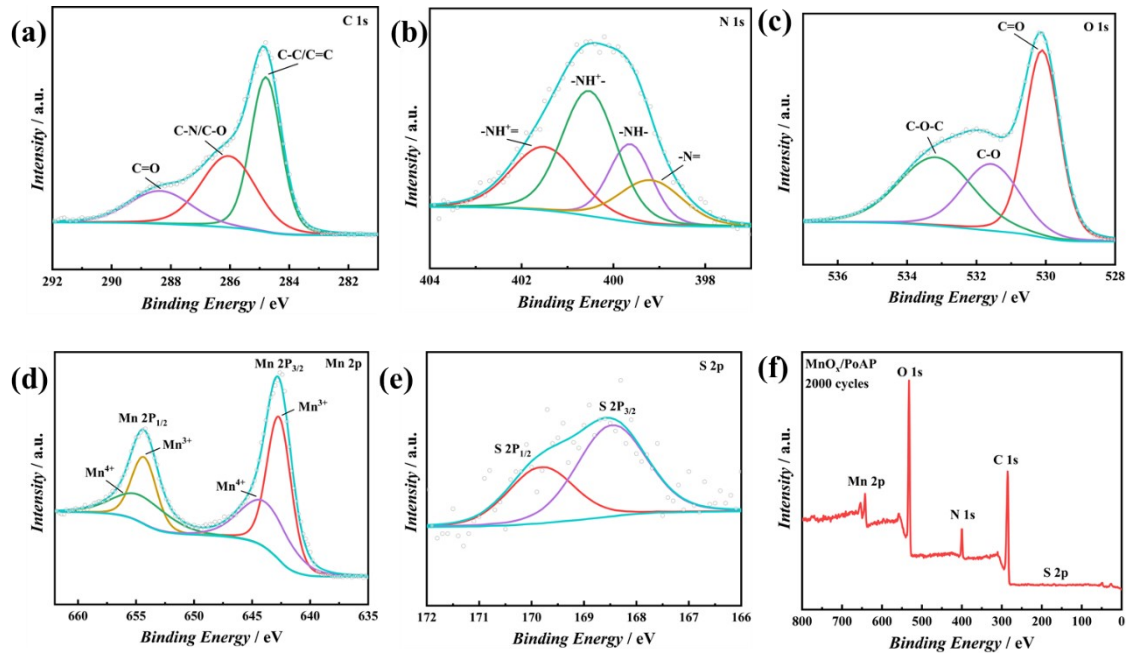

Figure S8. Deconvoluted high-resolution XPS spectra of the (a) C 1s region; (b) N 1s region; (c) O 1s region; (d) S 2p region; (e) Mn 2p region of the as-deposited MnO_x/PoAP; (f) after charge-discharge 2000 cycles in 2 M $(NH_4)_2SO_4$.

Table S1. Components of the deconvoluted C 1s XPS spectra of the MnO_x/PoAP-1.

	284.65 eV	286.15 eV	288.39 eV
	C-C/C=C	C-N/C-O	C=O
1 M H_2SO_4	37.83	45.05	17.12

Table S2. Components of the deconvoluted N 1s XPS spectra of the MnO_x/PoAP-1.

	399.40 eV	400.14 eV	400.80 eV	401.67 eV
	-N=	-NH-	$-NH^+-$	$-NH^+=$
1 M H_2SO_4	30.86	36.33	21.53	11.28

Table S3. Components of the deconvoluted O 1s XPS spectra of the MnO_x/PoAP-1.

	532.16 eV	533.33 eV	534.17 eV
	C=O	C-O	C-O-C
1 M H_2SO_4	72.38	14.46	13.17

Table S4. Components of the deconvoluted Mn 2p XPS spectra of the MnO_x/PoAP-1.

	642.17 eV	644.97 eV	653.76 eV	654.70 eV
	Mn^{3+}	Mn^{4+}	Mn^{3+}	Mn^{4+}
1 M H_2SO_4	46.75	22.49	16.92	13.84

Table S5. Components of the deconvoluted N 1s XPS spectra of the MnO_x/PoAP-1 charged or discharged in different solutions.

	399.51 eV **-N= (%)**	**400.03 eV** **-NH- (%)**	**400.70 eV** **-NH^+- (%)**	**401.12 eV** **-NH^+= (%)**
2 M $(NH_4)_2SO_4$ Charged	19.86	29.51	37.07	13.55
2 M $(NH_4)_2SO_4$ Discharged	2.58	57.03	34.68	5.71
2 M KCl Charged	4.08	7.3	54.92	33.7
2 M KCl Discharged	15.41	48.71	27.91	7.97

Table S6. Components of the deconvoluted O 1s XPS spectra of the MnO_x/PoAP-1 charged or discharged in different solutions.

	530.10 eV Mn-O-Mn (%)	**532.10 eV C=O/Mn-OH (%)**	**533.51 eV C-O (%)**	**534.21 eV C-O-C (%)**
2 M $(NH_4)_2SO_4$ Charged	7.64	50.48	27.86	14.02
2 M $(NH_4)_2SO_4$ Discharged	3.64	56.94	31.54	7.88
2 M KCl Charged	15.49	42.19	30.73	11.59
2 M KCl Discharged	4.77	43.76	36.94	14.53

Table S7. Components of the deconvoluted N 1s XPS spectra of the MnO_x/PoAP-1 charged or discharged in different solutions.

	642.33 eV	**644.83 eV**	**654.12 eV**	**655.71 eV**
	Mn^{3+} (%)	**Mn^{4+} (%)**	**Mn^{3+} (%)**	**Mn^{4+} (%)**
2 M $(NH_4)_2SO_4$ Charged	48.06	18.41	19.5	14.03
2 M $(NH_4)_2SO_4$ Discharged	48.39	22.04	26.32	3.25
2 M KCl Charged	39.47	25.97	9.72	24.83
2 M KCl Discharged	45.09	25.26	17.44	12.21

4. SEM

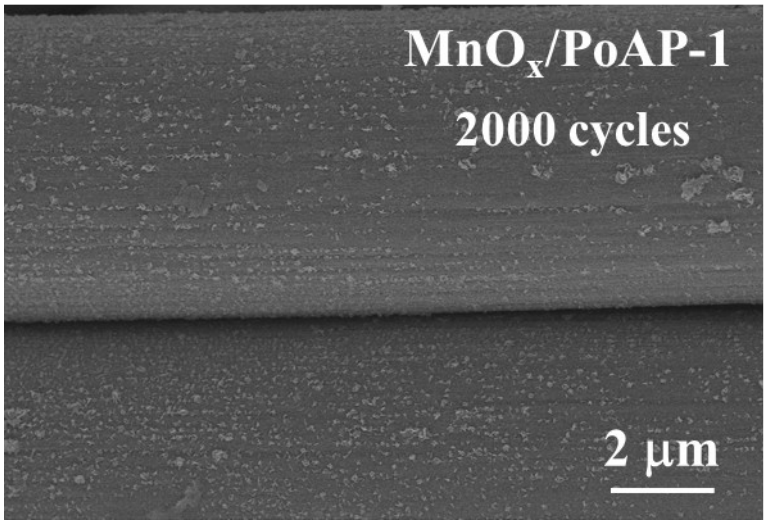

Figure S9. The SEM images of the MnO_x/PoAP-1 after GCD cycling at 10 A g^{-1} for 2000 cycles in 2 M $(NH_4)_2SO_4$.

5. Comparison of specific capacity and cyclic stability

Table S8. Comparison of specific capacity and cycling stability of conducting polymer/metal oxide composites.

Material	*Electrolyte*	*Specific capacity*	*Cyclic stability*	*Ref.*
MnO_x/PoAP	2 M $(NH_4)_2SO_4$	100.88 mAh g^{-1} at 1 A g^{-1}	92.58% after 10000 cycles	This work
	2 M KCl	166.94 mAh g^{-1} at 1 A g^{-1}	78.51% after 10000 cycles	
MnO_x(AAIC)	2 M $(NH_4)_2SO_4$	175 F g^{-1} at 1 A g^{-1}	89% after 1000 cycles	[1]
α-MnO_2/PANI/rGO	0.5 M H_2SO_4	77 F g^{-1} at 1 mA cm^{-2}	75% after 2000 cycles	[2]
V_2O_5@PPy	1 M Na_2SO_4	307 F g^{-1} at 1 A g^{-1}	82% after 1000 cycles	[3]

6. References

[1] S. G. Krishnan, H. D. Pham, C. Padwal, H. Weerathunga, X. Wang, K. Mahale and D. Dubal, Journal of Power Sources, 2023, 570, 232994.

[2] P. H. Patil, V. V. Kulkarni, T. D. Dongale and S. A. Jadhav, Journal of Composites Science, 2023, 7, 167.

[3] Y. Liang, Z. Wei, X. Zhang and R. Wang, ES Energy & Environment, 2022, 18, 101-110.